Catalysis Today 296 (2017) 118–126

Contents lists available at ScienceDirect

Catalysis Today

journal homepage: www.elsevier.com/locate/cattod

Reductive amination of levulinic acid to different pyrrolidones on Ir/SiO_2-SO_3H: Elucidation of reaction mechanism

José J. Martínez[a,*], Leonardo Silva[a], Hugo A. Rojas[a,*], Gustavo P. Romanelli[b], Lucas A. Santos[c], Teodorico C. Ramalho[c], María H. Brijaldo[d], Fabio B. Passos[d]

[a] Escuela de Ciencias Químicas, Facultad de Ciencias, Universidad Pedagógica y Tecnológica de Colombia UPTC, Avenida Central del Norte, Tunja, Boyacá, Colombia
[b] Centro de Investigación y Desarrollo en Ciencias Aplicadas "Dr. J.J. Ronco" (CINDECA), Departamento de Química, Facultad de Ciencias Exactas, UNLP-CCT-CONICET, Calles 47 N° 257, B1900 AJK, La Plata, Argentina
[c] Departamento de Química, Universidade Federal de Lavras, Campus Universitário, Lavras, MG, 37200-000, Brazil
[d] Departamento de Engenharia Química e de Petróleo, Universidade Federal Fluminense, R. Passos da Pátria, 156, Niterói, RJ, 24210-240, Brazil

ARTICLE INFO

Keywords:
Pyrrolidones
Sulfonic groups
Reductive amination

ABSTRACT

Levulinic acid (LA) transformation to different pyrrolidones via reductive amination was studied using an Ir/SiO_2-SO_3H catalyst in liquid phase. The effects of solvent, amine concentration, H_2 partial pressure, catalyst mass, and reuse were studied. The spent catalysts were evaluated by DRIFTS to obtain evidence of the interaction of levulinic acid with aniline on the catalyst surface. The sulfonic groups on SiO_2 improved the yield to pyrrolidones and avoided side reactions. A reaction mechanism is proposed where the reductive amination occurs between LA and amine towards an intermediate amine that is then cycled. The Gibbs free energy for the reaction mechanism was evaluated. Besides, the HOMO and LUMO of the amine reactants and intermediates using density functional theory (DFT) with the B3LYP-D3 method were theoretically determined to understand the rate-limiting and the cyclization steps.

1. Introduction

Levulinic acid (LA) is obtained by hydrolysis of cellulose, and its reductive amination is an interesting process because pyrrolidones are produced. In several industrial processes, pyrrolidones are important as solvents, surfactants, complexing agents, and as part of pharmaceutical formulations [1,2]. Recently, Zhu et al. [3] have demonstrated that the system composed of N-methyl-2-pyrrolidone and C1–C4 carboxylic acid can be used as a solvent with exceptional lignin solubility that outperforms conventional solvents and ionic liquids. Therefore, reductive amination has attracted considerable interest due to its potential to produce a variety of pyrrolidones [4]. Raney nickel catalysts or silica gel-supported nickel catalysts were used to transform LA to 1,5-methyl-2-pyrrolidone by reductive amination using high pressures of H_2 (1000–2000 Psi) [5,6]. Touchy et al. [7] studied different metal-supported catalysts to obtain aryl-, alkyl-, and cycloalkylpyrrolidones with the aim of increasing the catalytic activity for the reductive amination of LA. They used Pt and MoO_x coloaded TiO_2, which allows polarization of the carbonyl groups via Lewis acid−base interaction. However, these authors did not show evidence of this type of interaction. Wei et al. used transfer hydrogenation methods [8] or a noncatalytic system [9] with the aim of diminishing the high pressure or temperature employed in conventional hydrogenation processes. They found that the solvent DMSO is critical for the high reactivity observed. The reason why DMSO is an effective solvent is unclear. Andrioletti et al. [10] reported another example of metal-free reductive amination of LA. However, the reaction required more forceful conditions including higher temperatures (433–473 K) with the disadvantage of the formation of formamide as byproduct of the condensation of the formic acid and amine used. Table 1 summarizes the yield and recycle of catalysts reported in the literature to obtain 5-methyl-N-phenyl-2-pyrrolidone.

In this contribution, we studied the synthesis of some pyrrolidones from levulinic acid using Ir/SiO_2-SO_3H. The aim of this work is to determine the role of acid sites in the reductive amination of levulinic acid. The reductive amination of levulinic acid requires nucleophilic addition, which could be favored by the presence of Brönsted sites. To the best of our knowledge, this is the first time an Ir/SiO_2-SO_3H catalyst has been used in the reductive amination of levulinic acid.

* Corresponding authors.
E-mail addresses: jose.martinez@uptc.edu.co (J.J. Martínez), hurojas@udec.cl (H.A. Rojas).

http://dx.doi.org/10.1016/j.cattod.2017.08.038
Received 14 January 2017; Received in revised form 6 June 2017; Accepted 14 August 2017
Available online 19 August 2017

Table 1
Yield and recycle of catalysts to obtain 5-methyl-N-phenyl-2-pyrrolidone.

LA:A (mmol)	Catalyst	Solvent	Y (%)	Time (h)	Recycles	Ref.
1:1	Pt-MoOx/TiO_2	No solvent	90	20	Four cycles	[7]
3.3:8.6	Iridicycle catalyst	No solvent	91	1	Not evaluated	[8]
1:3	No catalyst	DMSO	34	12	No catalyst	[9]
1:1	t-Bu_3 $PHBF_4$	Toluene	> 70	12	Homogeneous catalyst	[11]
1:1	$In(OAc)_3$ and $PhSiH_3$	Toluene	94	24	Homogeneous catalyst	[12]
2:1	$[Ru_3(CO)_{12}]$	No solvent	93	12	Homogeneous catalyst	[13]

2. Experimental

2.1. Catalyst preparation

The Ir/SiO_2-SO_3H catalyst was previously prepared and characterized as described in reference [14]. Briefly, a mixture of 5 g SiO_2 (Syloid, S_{BET} = 283 m^2/g) in 100 mL of dry toluene (Panreac, 99.5%) and 3-mercaptopropyltrimethoxysilane (MPTMS; Sigma-Aldrich, 95%) (1.15 mL, 6.1 mmol) was refluxed for 24 h. The obtained solid was washed with toluene and dried at 363 K. Subsequently, mercaptopropyl groups were oxidized to sulfonic acid groups with excess hydrogen peroxide (30%, Panreac) at room temperature for 24 h. A few drops of H_2SO_4 were added during 12 h, and the solid was washed with acetone and dried at 393 K.

The solid SiO_2-SO_3H was then impregnated with Ir-PVP colloids (PVP: polyvinylpyrrolidone) at room temperature for 6 h under stirring and then dried under vacuum at 353 K. The synthesis of Ir-PVP colloids was similar to that described in the literature [15].

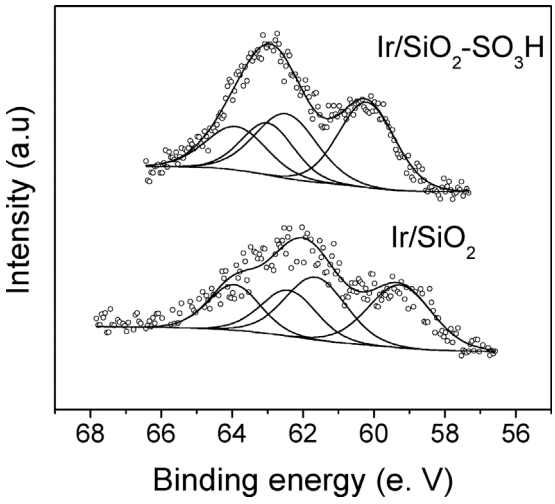

Fig. 2. XPS spectra of Ir/SiO_2-SO_3H and Ir/SiO_2 catalysts.

Table 2
Binding energies of Ir and IrO_2 in the solids studied and in Ir-bulk reported in the literature.

	Ir^0 $Ir4f_{7/2}$	Ir^0 $4f_{7/2}$	IrO_2 $4f_{7/2}$	IrO_2 $4f_{7/2}$
Ir/SiO_2	59.3	62.5	61.7	64.0
Ir/SiO_2-SO_3H	60.2	63.1	62.5	63.9
Ir-Bulk	60.8 [22]	63.8	62.9 [23]	65.9

2.2. Catalyst characterization

The Ir-PVP supported catalyst was characterized by X-ray photoelectron spectroscopy (XPS). XPS data were obtained in a Thermo

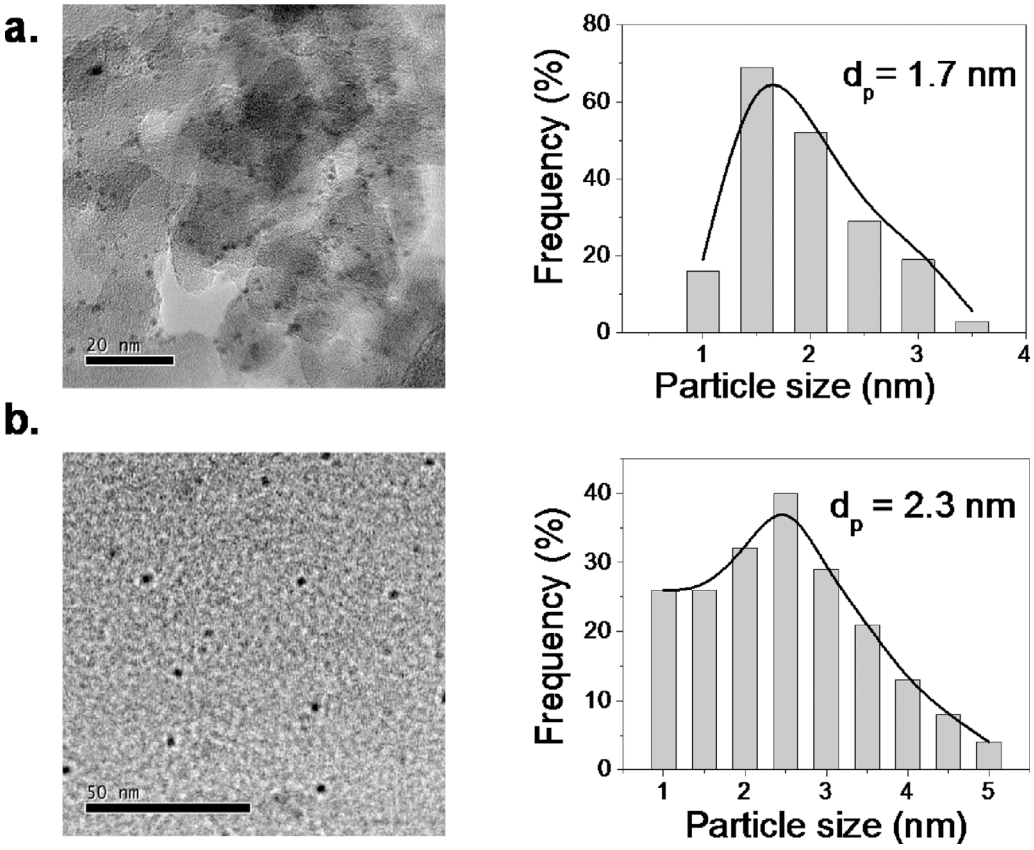

Fig. 1. Typical TEM images and particle size distribution of Ir catalysts (a) Ir/SiO_2 and (b) Ir/SiO_2-SO_3H.

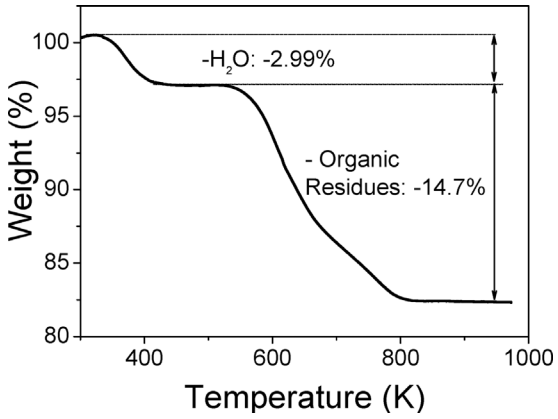

Fig. 3. Thermogram of Ir/SiO_2-SO_3H catalyst.

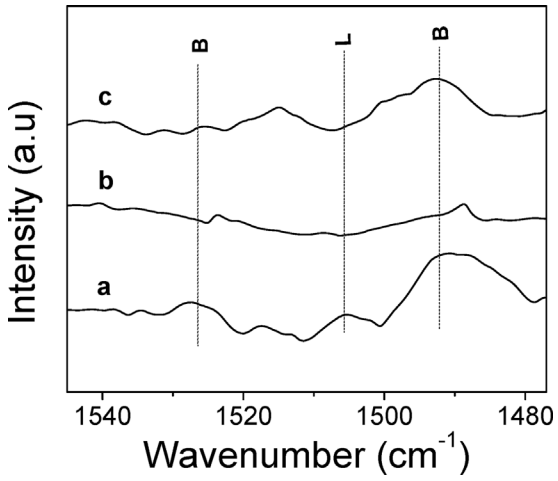

Fig. 4. FTIR-Pyr of: **(a).** SiO_2-SO_3H **(b).** Ir/SiO_2 and **(c).** Ir/SiO_2-SO_3H, where B and L are Brönsted and Lewis sites, respectively.

Table 3
Catalytic data obtained at 8 h of reaction in the reductive amination of levulinic acid with aniline, where $Y_{C=N}$ and $Y_{N\text{-}C}$ are the yield to imine and amine, respectively. Reaction conditions: 0.125 mol of LA and 0.25 mol of aniline at 373 K, 500 psi of H_2, 0.1 g of catalyst, ethyl acetate as solvent.

Catalyst	Conversion (%)	$Y_{C=N}$ (%)	$Y_{N\text{-}C}$ (%)
Blank	0	0	0
SiO_2-SO_3H	50	50	0
Ir/SiO_2	6	0	6
Ir/SiO_2-SO_3H	63	0	63

Scientific Escalab 250 XI spectrometer. The samples were purged with helium (25 mL/min) for 1 h in the chamber of analysis. Measurements were performed at room temperature with monochromatic Al Kα ($h\nu$ = 1486.6 eV) radiation. The analyzer was operated at 25 eV pass energy with a step size of 0.05 eV. The pressure in the analytical chamber was 6.3×10^{-9}mBar. The C 1 s signal (284.6 eV) was used as internal energy reference in all the experiments. Core-level peak positions were determined after background subtraction according to Shirley method using Avantage software. Peaks in a spectrum were fitted by a combination of Gauss and Lorentz curves, and overlapping peaks were also separated using this combination.

Iridium particle size was determined by transmission electron microscopy in a JEOL JEM-1011 analytical microscope. At least 200 particles were measured to obtain the particle size distribution and the average particle size d_p defined as $d_p = \Sigma nidi^3/\Sigma nidi^2$, where ni represents the number of particles with a diameter di.

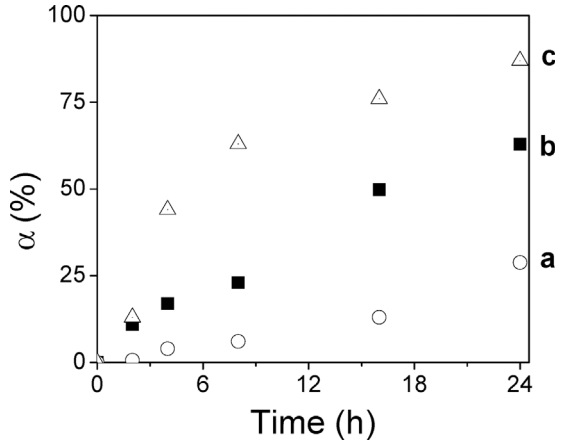

Fig. 5. Conversion level as a function of reaction time in the reductive amination of levulinic acid using **(a)** SiO_2SO_3H and **(b)** Ir/SiO_2, and **(c)** $IrSiO_2$-SO_3H. Reaction conditions: 0.125 mol of LA and 0.25 mol of aniline at 373 K, 500 psi of H_2, 0.1 g of catalyst, ethyl acetate as solvent.

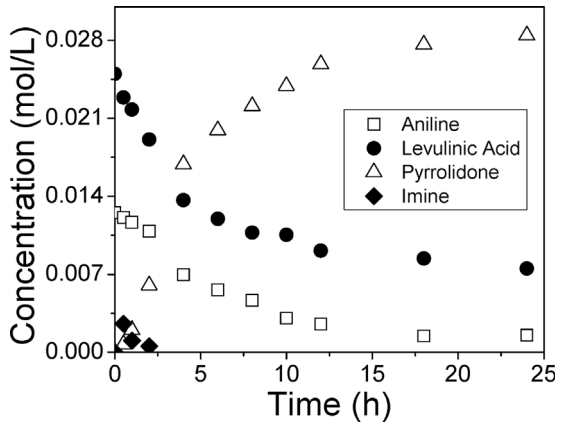

Fig. 6. Catalytic activity of the reductive amination of levulinic acid with aniline, using Ir/SiO_2-SO_3H catalyst. Reaction conditions: 0.125 mol of LA and 0.25 mol of aniline at 373 K, 500 psi of H_2, 0.1 g of catalyst, ethyl acetate as solvent.

Table 4
Effect of catalyst mass on the yield to pyrrolidone in the reductive amination of levulinic acid with aniline. Reaction conditions: 0.125 mol of LA and 0.25 mol of aniline at 373 K, 500 psi of H_2, 0.1 g of catalyst, ethyl acetate as solvent.

Catalyst mass (g)	r_0 (mol/m^3 s)	N_{WP}
0.01	0.0014	2.3×10^{-6}
0.05	0.0011	1.7×10^{-6}
0.1	0.0010	1.2×10^{-6}

Table 5
Effect of aniline:LA molar ratio on pyrrolidone yield at 8 h of reaction. Reaction conditions: 373 K, 500 psi of H_2, 0.1 g of catalyst, ethyl acetate as solvent.

Molar ratio of aniline: LA	α (%),	$Y_{C=N}$ (%)	$Y_{N\text{-}C}$ (%)
0.125:0.250	63	–	63
0.250:0.250	18	–	18
0.250:0.125	4	–	4

Thermogravimetric analysis (TGA) was performed in SETARAM SA equipment, using a heating rate of 5 K·min^{-1} from room temperature to 1073 K in inert atmosphere.

The nature of acid sites was studied by pyridine (Pyr) adsorption followed by FTIR. Infrared spectra were collected using Nicolet iS50 equipment with an in situ diffuse reflectance cell (Harrick, Praying

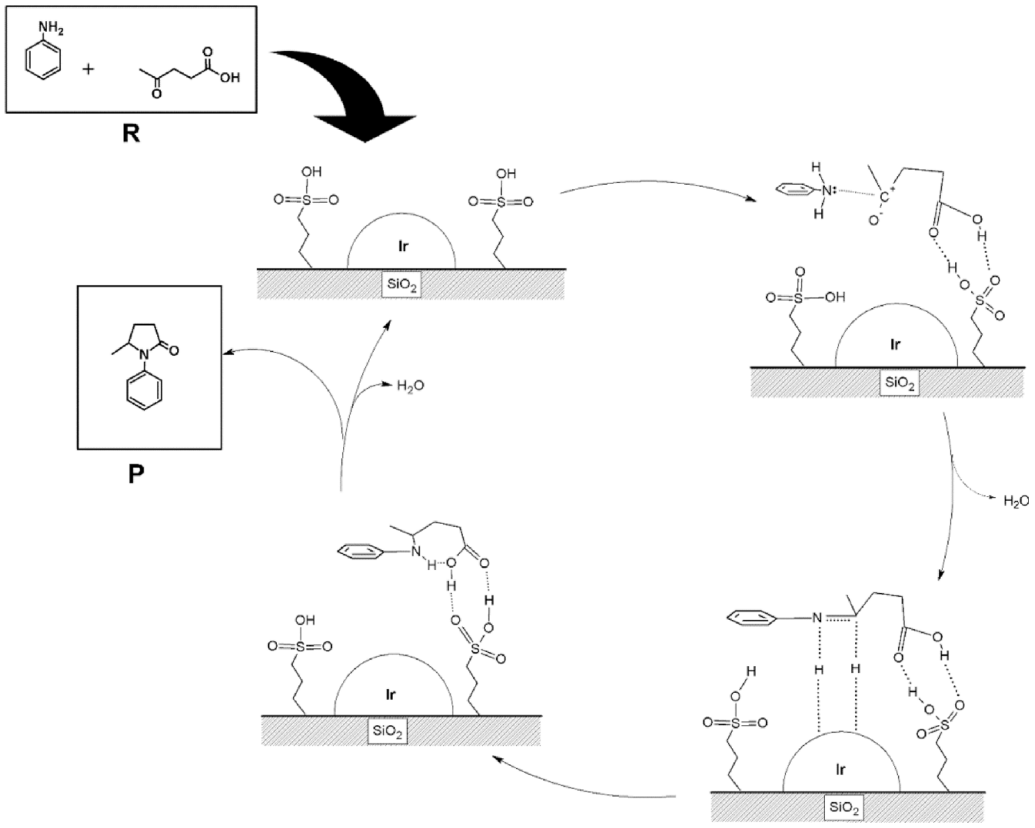

Fig. 7. Plausible mechanism for the reductive amination of levulinic acid with aniline over Ir/SiO_2-SO_3H catalyst.

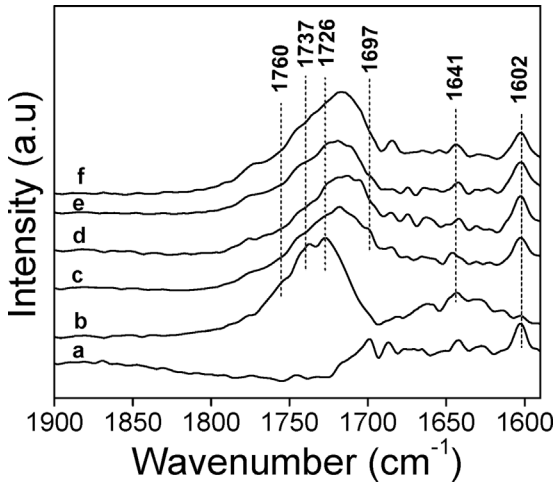

Fig. 8. DRIFT spectra of Ir-SiO_2 at different reaction times. (a): Adsorption of aniline, and (b): adsorption of levulinic acid on the catalyst surface. Spectra a and b are considered as time zero. (c), (d), (e), and (f): DRIFT spectra of the spent catalyst at 15, 30, 60 and 90 min of reaction, respectively.

Mantis). For the determination of acid sites, a pretreatment at 423 K was performed with a helium flow of 15 mL/min for 1 h to clean the surface of possible contaminants. Subsequently, the samples were gradually cooled down to 303 K, and then pyridine adsorption was performed for 1 h. After adsorption, the gas phase was removed by evacuation with a helium flow (20 mL/min).

DRIFT spectra of the spent catalyst were collected at different times of reaction. The catalyst was separated by filtration, dried, and placed in a Harrick cell. The cell was purged with helium at a constant flow of 50 mL/min at 373 K before collecting the spectrum.

Table 6
Effect of partial pressure of H_2 at 8 h of reaction using Ir/SiO_2-SO_3H catalyst in the range of 250–700 psi. Reaction conditions: 0.125 mol of LA and 0.25 mol of aniline at 373 K, 0.1 g of catalyst, ethyl acetate as solvent.

H_2 Pressure (psi)	α (%)	$Y_{C\text{-}N}$ (%)	$Y_{C=N}$ (%)
250	62	62	–
500	63	63	–
750	24	24	–

Table 7
Effect of solvent on the reductive amination of levulinic acid with aniline. Reaction conditions: 0.125 mol of LA and 0.25 mol of aniline at 363 K, 500 Psi of H_2, and 0.1 g of Ir/SiO_2SO_3H catalyst.

Solvent	α (%)	$Y_{C\text{-}N}$ (%)	$Y_{C=N}$ (%)	Y_{other} (%)
Ethanol	54	20	–	34 (m/z = 144.2)
Acetonitrile	19	19	–	–
Ethyl acetate	63	63	–	–

2.3. Catalytic tests

The liquid phase reductive amination reaction was carried out in a batch-type reactor at constant stirring rate (1000 rpm) using 40 mL of 0.125 M aniline solution and 0.250 M levulinic acid solution, in ethyl acetate as solvent, using 0.1 g of Ir/SiO_2-SO_3H catalyst, at a reaction temperature of 373 K. The effect of H_2 pressure on the reductive amination of levulinic acid was studied at a H_2 pressure ranging from 250 to 750 Psi. The Weisz–Prater criterion was employed to assess the influence of the intraparticle diffusion resistance criterion. Reaction products were analyzed in a gas chromatograph coupled to a mass spectrometer (GC–MS) Varian 3800-Saturn 2000 furnished with a β-Dex column, helium as carrier, and constant temperature at 393 K. The

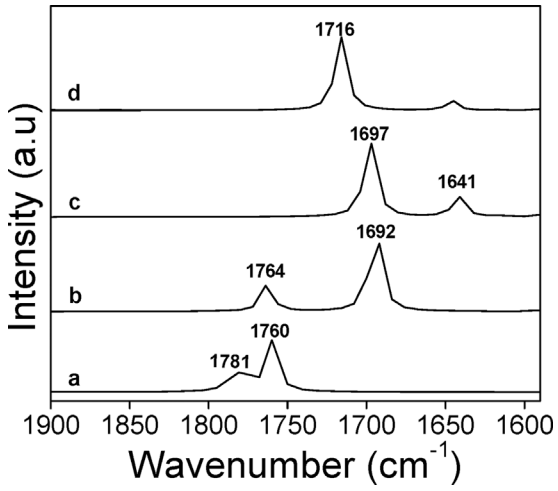

Fig. 9. Theoretical IR (a) levulinic acid, (b) levulinic acid adsorbed on Ir/SiO_2-SO_3H, (c) step II product (hydrogenation product interacting with $-SO_3H$ groups), and (d) final product of reaction.

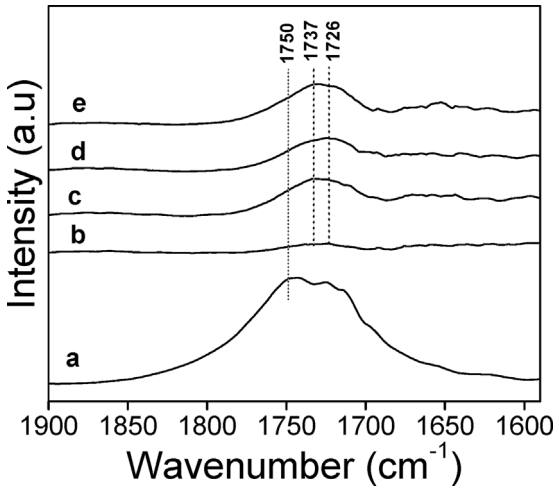

Fig. 10. DRIFT spectra of Ir-SiO_2 at different reaction times. (a) Adsorption of levulinic acid on the catalyst surface. Spectra a and b are considered as time zero. (c), (d), (e), and (f): DRIFT spectra of the spent catalyst at 15, 30, 60 and 90 min of reaction, respectively.

conversion of substrate (levulinic acid) and selectivity to pyrrolidone were determined using Eqs. (1) and (2). The conversion of reactant (α) and product yield (Y) and selectivity were defined as follows:

$$\alpha(\%) = \frac{C_0 - C_i}{C_0} 100 \quad (1)$$

$$S(\%) = \frac{C_{ptod}}{\sum C_{ptos}} 100 \quad (2)$$

$$Y = S^{*}\alpha \quad (3)$$

where C_0 is the initial concentration, C_i is the concentration at time *i*, C_{ptod} is the concentration of the desired product, and C_{ptos} is the concentration of the obtained products. $Y_{N=C}$ and $Y_{N\text{-}C}$ are yield to imine or yield to pyrrolidone, respectively.

Different pyrrolidones were synthesized by changing the amine molecule. Its identification was performed by comparison of the *m/z* spectra, because they are not new compounds, except for pyrrolidone derived from furfurylamine.

(i) *5-Methyl-N-phenyl-2-pyrrolidone:* Yield: 63%; *m/z* calc.: 175.2. Found: 175.2.
(ii) *5-Methyl-1-p-tolyl-pyrrolidin-2-one:* Yield: 43%; *m/z* calc.: 189.257. Found: 189.3.
(iii) *1-(4-Chlorophenyl)-5-methylpyrrolidin-2-one:* Yield: 31%; *m/z* calc.: 209.675. Found: 210.
(iv) *5-Methyl-1-(3-nitro-phenyl)-pyrrolidin-2-one:* Yield: 3%; *m/z* calc.: 220.228. Found: 220.3.
(v) *N-benzyl-5-methylpyrrolidin-2-one:* Yield: 31% (lit. [16])
(vi) *1-(4-Aminophenyl)-5-methylpyrrolidin-2-one:* Yield: 46%; (lit. [12]); *m/z* calc.: 191.22642. Found: 191.23.
(vii) *1-(Furan-2-ylmethyl)-5-methyl-pyrrolidin-2-one:* Yield: 39%; *m/z* calc.: 179.216. Found: 179.5.

2.4. Computational details

2.4.1. Determination of HOMO and LUMO

The geometries of the molecules in the gas phase were optimized at the B3LYP/6–31 + +** level with Grimme's D3 empirical dispersion correction using the Gaussian 09 software [17], in order to obtain the HOMO and LUMO energies of the anime reactants and intermediates. The structures were minimum on potential energy surface, and their harmonic vibrational frequencies were positive. Molecule visualizations at their optimized geometries and ionization potential surfaces were performed using the MacMolPlt program package.

2.4.2. Thermodynamic analysis

The optimized geometries of each reaction step and their correspondent Gibbs free energies in ethyl acetate at 363 K were calculated at the B3LYP/6–31 + +** level with Grimme's D3 empirical dispersion correction [18], using the Gaussian 09 software [17]. The solvation environment was simulated using/employing the polarizable continuum model (PCM) [19].

The transition state calculations of the hydrogenation step were carried out at B3LYP-D3/lanL2DZ level. The iridium nanoparticles were modeled using the Ir unit cell coordinates imported from materialsproject.org [ID: mp-101].

2.5. Reuse of catalyst

The catalytic activity of the reductive amination of levulinic acid with aniline was studied for 4 cycles. After a typical reaction, the Ir/SiO_2-SO_3H catalyst was filtered with a Whatman® cellulose filter paper − (Sigma-Aldrich), and dried at 373 K for 1 h.

3. Results and discussion

3.1. Catalyst characterization

Fig. 1 displays typical TEM images and the corresponding particle size distribution histograms for Ir/SiO_2 and Ir/SiO_2-SO_3H catalysts. The average particle size d_p was 1.7 nm for Ir/SiO_2, while for Ir/SiO_2-SO_3H it was 2.3 nm. The particle size distribution was broader on Ir/SiO_2-SO_3H support, possibly due to some interaction between the sulfonic groups and the PVP used as stabilizing on Ir colloids. This phenomenon does not occur when metal particles are deposited without surfactant as in the case of Ru/SiO_2-SO_3H [20].

Fig. 2 show the deconvoluted XP spectra of Ir/SiO_2 and Ir/SiO_2-SO_3H in the region of Ir 4f. The binding energies (BE) of Ir $4f_{7/2}$ and $4f_{5/2}$ peaks are summarized in Table 2. Both contributions of Ir 4f are associated with Ir^0 atoms and partially oxidized IrO_2, respectively. BE values are slightly smaller than the corresponding values of the bulk for Ir^0. In both cases (Ir/SiO_2 and Ir/SiO_2-SO_3H), the corresponding values can be attributed to electron donation from the PVP [14], which makes the Ir particles slightly negatively charged [21]. This phenomenon is most evident in the Ir/SiO_2 catalyst. Thus, it seems that the sulfonic groups have some interaction with PVP, altering the chemical environment of the metal particles. In addition, peaks assignable to IrO_2 were also slightly smaller than the corresponding bulk values.

Thermogravimetric analyses (TGA) were performed to corroborate

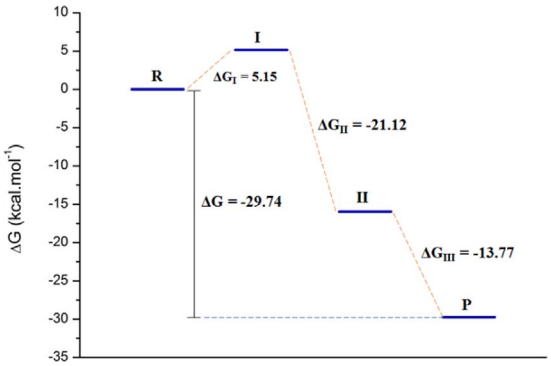

Fig. 11. Thermodynamic details following the three steps proposed for the reaction mechanism from the reactants (R) to the products (P).

the temperature of decomposition of organic residues. Fig. 3 shows the TGA of Ir/SiO_2-SO_3H catalyst. The loss of H_2O can be observed at 393 K. However, the loss of organic residues (associated with MPTMS, sulfonic groups, and PVP) can be seen from 550 K to 820 K, confirming that the catalyst structure is preserved at the reaction temperatures.

In order to determine the acid site nature of catalysts, pyridine-FTIR analysis was performed (Fig. 4). In SiO_2-SO_3H three bands at 1490 cm^{-1}, 1503 cm^{-1} and 1531 cm^{-1} can be observed. The bands at 1490 cm^{-1} and 1531 cm^{-1} are associated with typical Brönsted sites. The band at 1503 cm^{-1} is characteristic of Lewis acid sites [24,25]. The Pyr-FTIR spectrum of Ir/SiO_2-SO_3H only shows the bands associated with Brönsted sites. Ir/SiO_2 catalyst does not present Brönsted sites.

3.2. Catalytic tests

Levulinic acid with aniline was studied as test reaction, and blank experiments were carried out to study the effect of the sulfonic groups (Table 3). Fig. 5 shows the conversion level as a function of reaction time in the reductive amination of levulinic acid. The plateau only seems to be reached in the test with Ir/SiO_2-SO_3H catalyst with a conversion near 90% at 24 h. The Ir/SiO_2 catalysts shows the lowest conversion.

With regard to selectivity, the hydrogenation of both carbonyl groups of levulinic acid was not observed in any catalyst. When SiO_2-SO_3H was used as catalyst, imine was the only product observed. By using the Ir/SiO_2 catalyst, the reaction proceeds to pyrrolidone with a lower yield at the time of reaction studied. The pyrrolidone yield increased when the Ir/SiO_2-SO_3H catalyst was used. Due to this fact, pyrrolidone was the only product obtained in the Ir catalysts; the activity was compared at 8 h, and it was expressed as yield to imine ($Y_{C=N}$ (%)) or yield to pyrrolidone ($Y_{N\text{-}C}$ (%)). Table 3 summarizes the catalytic data obtained at 8 h of reaction.

Fig. 6 shows the evolution of levulinic acid and aniline concentration and their products in time using Ir/SiO_2-SO_3H catalyst. It is noted that imine formation takes place mainly during the first 2 h of reaction and it is not detected at high/long reaction times. Thus, the hydrogenation is fast. Pyrrolidone is the main product of reaction, and other products were not observed.

The best reaction conditions for the reductive amination of levulinic acid with aniline were: constant stirring rate (1000 rpm) using 40 mL of 0.125 M aniline solution and 0.250 M levulinic acid solution, with ethyl acetate as solvent, at a reaction temperature of 373 K, with a hydrogen pressure of 500 psi, using 0.1 g of Ir/SiO_2-SO_3H catalyst.

3.2.1. Effect of catalyst mass

The effect of catalyst loading on the yield to pyrrolidone in the catalytic reductive amination of LA was studied. The results are listed in Table 4, and they lead us to believe that there is a linear trend in the yield to pyrrolidone with an increase of the catalyst mass used. This suggests an absence of external mass transfer resistance. The Weisz–-Prater criterion was employed to assess the influence of intraparticle diffusion resistance. Table 4 shows the Weisz- Prater values at distinct mass used. In all cases, the value of the Weisz-Prater (N_{WP}) criterion calculated was less than 1. Hence, there was no intraparticle diffusion resistance.

3.2.2. Effect of amine concentration and H_2 partial pressure

The role of sulfonic groups favors the adsorption of LA and could also allow adsorption of the amine molecule, causing a possible decrease of the yield to pyrrolidone. Thus, the surface coverage by amines inhibits the adsorption of LA step, and this could cause the formation of an amine salt (-SO_3H + RNH_2 = SO_3-NRH_3^+). The above-mentioned can be observed in Table 5, as the highest aniline: LA ratio inhibits the formation of pyrrolidone. This fact was observed by the band at

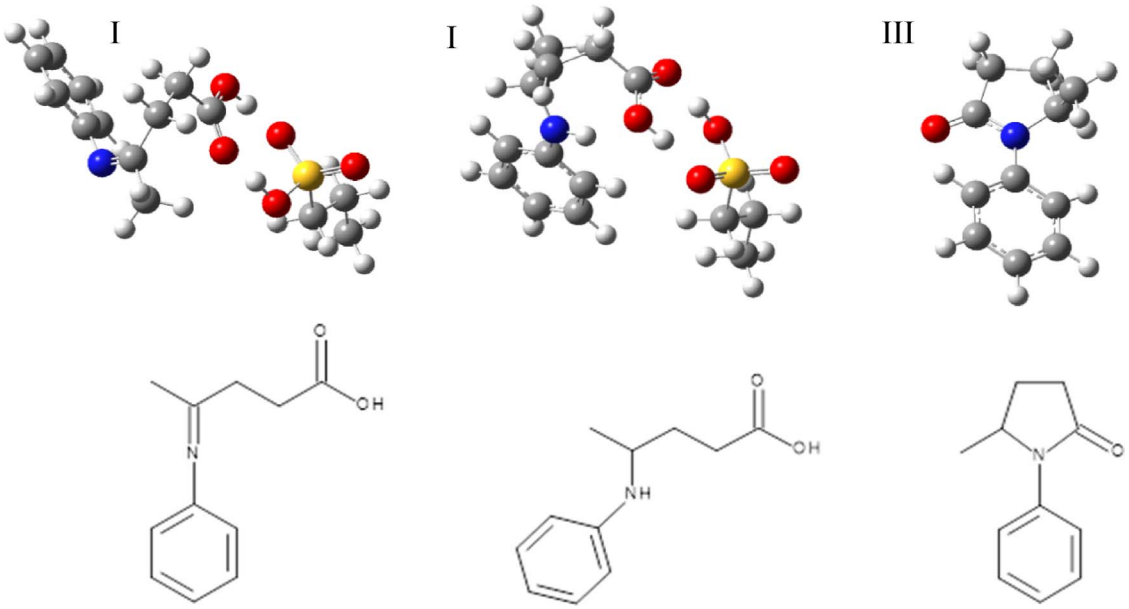

Fig. 12. Theoretical geometries of the first (I), second (II) and third (III) step products. Color code: carbon in gray, hydrogen in white, nitrogen in blue, oxygen in red, and sulfur in yellow. (For interpretation of the references to colour in this figure legend, the reader is referred to the web version of this article.)

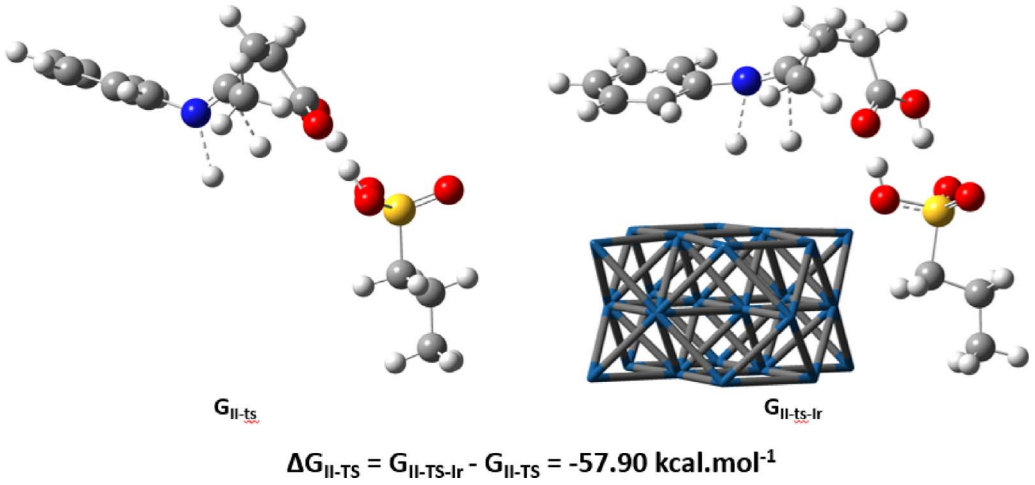

Fig. 13. Comparison between step II transition states with ($G_{II\text{-}ts\text{-}Ir}$) and without ($G_{II\text{-}ts}$) iridium nanoparticles. Color code: carbon in gray, hydrogen in white, nitrogen in blue, oxygen in red, and sulfur in yellow. The IR nanoparticles are represented by the blue and dark gray tubes. (For interpretation of the references to colour in this figure legend, the reader is referred to the web version of this article.)

1602 cm^{-1} in the IR spectra of the spent catalysts (see Fig. 8).

The effect of H_2 pressure on the reductive amination of levulinic acid was studied in the range of 250–750 psi at constant initial concentration. The results of different partial pressures of hydrogen are listed in Table 6. An increase in hydrogen pressure caused a decrease in the conversion and yield of pyrrolidone. This could be explained by a small interaction of amine molecules on the catalyst surface with an increase in H_2 pressure.

3.2.3. Effect of solvent

We also studied the effect of solvent, and the results are summarized in Table 7. Pyrrolidone is the only product when the solvent reaction is acetonitrile and ethyl acetate. In ethanol, a lower yield to pyrrolidone is observed because of the competition of the reductive amination with the esterification between LA and ethanol (63%), producing a compound with m/z = 144.2.

3.2.4. Plausible mechanism of the reductive amination of levulinic acid

In line with the above findings, we propose a plausible mechanism (Fig. 7) for the reductive amination of levulinic acid with aniline over Ir/SiO_2-SO_3H catalyst based on the following assumptions:

1. The sulfonic groups interact with the carboxylic group of levulinic acid. An effective inductive effect on the CO group at that distance is not possible. The COOH-SO_3H- interaction only allows the carbonyl group C2 to be available for the nucleophilic addition and formation of imine.
2. The second step includes the C═C bond hydrogenation of imine by hydrogen on iridium nanoparticles to obtain the amine intermediate. This step results in the formation of the amine intermediate.
3. In the third step, the cyclization of the amine intermediate with the carboxyl group of levulinic acid occurs. This step also involves a nucleophilic attack of the amine intermediate with the carboxylate adsorbed on $-SO_3H$ groups, this reaction being spontaneous. This step occurs easily between the nitrogen atom (HOMO) and the carboxyl group (LUMO). The substituents alter the contribution HOMO − LUMO and consequently modify the yields obtained.

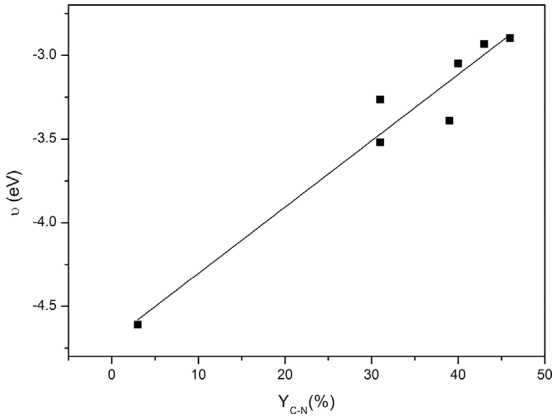

Fig. 14. Relation between the electronic chemical potential of the amine reactants and the yield (%) to pyrrolidones. Y = −4.6992 + 0.0396X, R^2 = 0.9472.

To confirm this plausible mechanism, DRIFT spectra of spent catalysts at different times of reaction and theoretical calculations were obtained.

Fig. 8a and b show the DRIFT spectra in the region of 1900–1590 cm^{-1} of aniline and LA adsorbed on the catalyst surface, respectively. In Fig. 8a, the band at 1602 cm^{-1} can be ascribed to the amine group scissoring vibration in anilinium sulfate, which has been previously assigned [26]. In Fig. 8b the band has two shoulders, one at 1737 cm^{-1} and other at 1726 cm^{-1}, which could be ascribed to the interaction of COOH groups and the carbonyl group of levulinic acid with sulfonic groups. The band at 1737 cm^{-1} could be attributed to C═

Table 8
Effect of amine substituent on the reductive amination of levulinic acid. Data of HOMO and LUMO energies and the electronic chemical potential (μ) of the amine reactants (ar). The band gap (BG) between HOMO and LUMO of the anime intermediates (ai).

Entry	Amine used	Yield (%) to pyrrolidone*	$HOMO_{ar}$ (eV)	$LUMO_{ar}$ (eV)	Electronic chemical potential μ_{ar} (eV)	BG_{ai} (eV)
i	*Aniline*	40	−5.7190	−0.3769	−3.0479	5.9726
ii	*p-Toluidine*	43	−5.5272	−0.3371	−2.9322	5.4202
iii	*p-Chloroaniline*	31	−5.8474	−0.6808	−3.2641	5.1835
iv	*m-Nitroaniline*	3	−6.4646	−2.7564	−4.6105	4.1441
v	*Benzylamine*	31	−6.5416	−0.4974	−3.5195	5.8365
vi	*p-Aminophenol*	46	−5.3519	−0.4416	−2.8968	4.9713
vii	*Furfurylamine*	39	−6.3693	−0.4101	−3.3897	6.544

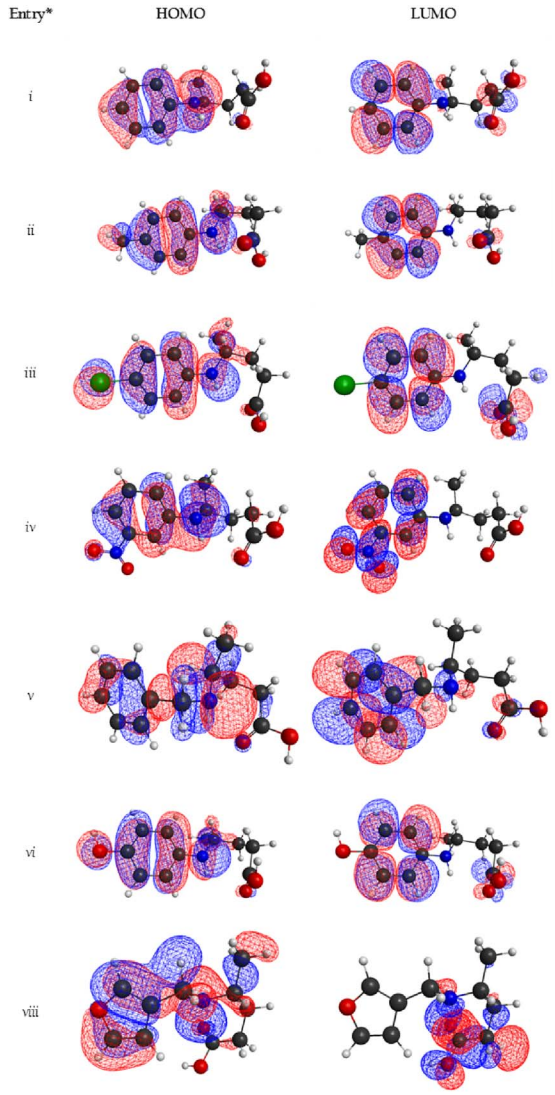

Fig. 15. Pictorial view of the HOMO and LUMO orbitals of amine intermediates. * Amine used/amine intermediate: (i) Aniline/4-phenylazanylpentanoic acid; (ii) *p*-toluidine/4-[(4-methylphenyl)amino] pentanoic acid; (iii) *p*-chloroaniline/4-[(4-chlorophenyl) amino]pentanoic acid; (iv) m-nitroaniline/4-[(4-nitrophenyl)amino]pentanoic acid; (v) benzylamine/4-[(phenylmethyl)amino]pentanoic acid; (vi) *p*-aminophenol/4-[(4-hydroxyphenyl)amino]pentanoic acid; (vii) furfurylamine/4-(furan-2-ylmethylamino)pentanoic acid.

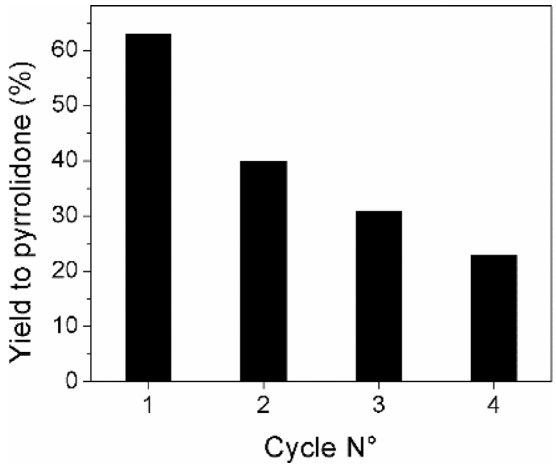

Fig. 16. Catalyst recycles at optimized reaction conditions.

O bond stretching and angular deformation of the C−O−H bond of the COOH group, which are described by the band at 1692 cm^{-1} in the theoretical spectrum (Fig. 9a). The other band at 1760 cm^{-1} is ascribed to C═O bond stretching of the carbonyl group, in agreement with the band at 1764 cm^{-1} in the theoretical spectra of levulinic acid adsorbed on Ir/SiO_2-SO_3H (Fig. 9b).

The spectra collected in the case of the spent catalyst at 15–90 min of reaction (Fig. 8c −8f) showed a shift of the adsorption bands of levulinic acid to lower wavenumbers, so the blue shift indicates a modification in the structure of levulinic acid as a consequence of aniline addition. In this spectrum, a band at 1641 cm^{-1} related to C−C bond stretching of the aromatic ring (which is also observed in the experimental spectra) is evidenced, while the band at 1697 cm^{-1} is characteristic of C═O bond stretching and angular deformation of the C−O−H bond of the COOH group. This was confirmed with the DRIFT theoretical spectrum of the step II product (Fig. 9c).

Comparing the data of the levulinic acid adsorbed on Ir/SiO_2-SO_3H (8b) and Ir/SiO_2 (Fig. 10a), there is a blue shift when the interactions with the SO_3H group take place. In Ir/SiO_2 (Fig. 10a), the proportion of the bands of LA adsorption change, a band at 1750 cm^{-1} being more predominant and possibly associated with the −COOH group vibrations (theoretical data points of the −COOH group vibrations of levulinic acid occur at 1760 cm^{-1}), which means that in Ir/SiO_2 more −COOH groups are available (i.e., not adsorbed). With progress of the reaction, the bands at 1750 cm^{-1} (Fig. 10b–e) decrease due to formation of the product (Fig. 9d).

In order to shed some more light on the experimental data, thermodynamic study about the stability of the intermediates was performed. In fact, the theoretical calculations emphasize the possibility of the proposed mechanism. Fig. 11 shows the Gibbs free energy of the mentioned steps, and the global ΔG is equal to −29.74 $kcal.mol^{-1}$. All calculated structures of each step are depicted in Fig. 12. In the first step (I), when imine formation occurs, the Gibbs free energy is 5.15 $kcal.mol^{-1}$. Despite this, the following steps are all spontaneous. The hydrogenation step (II) results in a stabilization of −21.12 $kcal.mol^{-1}$. This step is the most crucial to the whole reaction, with the lowest ΔG among the three steps. Here, the proposed mechanism suggests an interaction between the hydrogens and the iridium nanoparticles. In this sense, we calculated the transition state of step II with and without Ir atoms. In fact, the stabilization of the transition state in step II deserves some attention. Our calculations have shown that the difference between the activation energies with ($G_{II\text{-}TS\text{-}Ir}$) and without ($G_{II\text{-}TS}$) iridium nanoparticles is −57.90 $kcal.mol^{-1}$ (Fig. 13). Thus, the contribution of iridium nanoparticles to active hydrogen availability is very important. The third and final step (III) leads to the products with ΔG_{III} = −13.77 $kcal.mol^{-1}$.

3.2.5. *Effect of amine substituent*

The reductive amination of LA was carried out under optimized conditions, using a variety of aromatic amines and furfurylamine. The highest conversions were obtained with electron-donor substituents (entries ii and vi); however, by using electron-withdrawing groups (entry iv), the reaction is not favored (Table 8).

In order to clarify these phenomena, we correlated the activity and the molecular orbital properties of amine reactants in the first step of the proposed mechanism. This step is the most crucial to the mechanism, as our thermodynamic analysis has shown. Furthermore, we theoretically studied the HOMO and LUMO of amine intermediates formed to understand the cyclization step.

To compare the catalytic performance between all amine reactants, the electronic chemical potential (μ) was calculated using the HOMO − LUMO energies defined by Parr and Pearson [27] considering the equation: $\mu = -½ (I + A) = ½ (E_{HOMO} + E_{LUMO})$; where A is electron affinity (A), and I is ionization energy. The data of Table 8 show a relation between the electronic chemical potential of the amine intermediates and the yield (%) to pyrrolidones. Electron-withdrawing

groups decrease the HOMO energies, whereas they are increased by the presence of electron-donor groups. In fact, the substituent effect will affect the nucleophilic attack of the amine nitrogen on the carboxyl group, i.e., a higher electronegativity of amine reactants favors the first step effectiveness (see Fig. 14).

The pictorial view of the HOMO and LUMO in the amine intermediates (compounds *i-vii*) is depicted in Fig. 15. The HOMO shows a contribution from the nitrogen and benzene ring (or furan ring) and a very small contribution of the methyl group, whereas the LUMO corresponds mainly to the benzene ring and the carboxyl group. The cyclization step occurs easily between the nitrogen atom and the carboxyl group due to the interaction HOMO − LUMO, respectively. Albeit with the lowest band gap, when the substituent is *m*-nitroaniline, the carboxyl group does not contribute to the LUMO, and the yield to pyrrolidone is much lower (Table 7).

3.2.6. Reuse of catalyst

The catalyst reuse was studied in 4 cycles (Fig. 16). In this study, the catalyst was recovered, and not regenerated, to evaluate its behavior with the recycles. Thus, a progressive use of the catalyst in this reaction generates a loss of catalytic activity, due to saturation of $-SO_3H$ sites by the amine. The interaction of amine molecules with sulfonic groups allows the saturation of these sites. If the catalyst is not regenerated, amines adsorption is responsible for deactivation.

4. Conclusions

Levulinic acid transformation via reductive amination to pyrrolidones was studied using a bifunctional metallic-acidic catalyst in a liquid phase. The catalytic test of this reaction showed a yield to pyrrolidone higher than 60%, with a selectivity of 100%, using aniline as initial substrate and ethyl acetate as solvent. Although the max yield reported in this reaction is near 90%, reached in 20 h with Pt-MoOx/TiO_2, with our Ir/SiO_2-SO_3H catalyst it is 88% at 24 h. We propose a reaction mechanism where the carboxyl group is adsorbed on sulfonic groups favoring the formation of imine, which is then hydrogenated. This mechanism was corroborated with theoretical thermodynamic calculations and experimental results. The electronegativity (μ) of amine intermediates determines the cyclization step, mainly due to the interaction HOMO − LUMO between the nitrogen atom and the carboxyl group, respectively.

Acknowledgments

The authors thank Colciencias (Colombia) for financial support under the project 110965843004. Contract: Colciencias-UPTC 047-2015 and the project European Research Area Network; ERANet LAC (ref. ELAC2014/BEE-0341).

References

[1] L.E. Manzer, Production of 5-methyl-N-(methyl aryl)-2-pyrrolidone, 5-methyl-N-(methyl cycloalkyl)-2-pyrrolidone and 5-methyl-N-alkyl-2-pyrrolidone by reductive amination of levulinic acid with cyano compounds, US 6,841,520 B2, 2005.
[2] L.E. Manzer, F.E. Herkes, Production of 5-methyl-1hydrocarbyl-2-pyrrolidone by reductive amination of levulinic acid, US2004/0192933, 2004.
[3] L. Mu, Y. Shi, L. Chen, T. Ji, R. Yuan, H. Wang, J. Zhu, [N-Methyl-2-pyrrolidone][C1-C4 carboxylic acid]: a novel solvent system with exceptional lignin solubility, Chem. Commun. 51 (2015) 13554–13557.
[4] J.D. Vidal, M.J. Climent, P. Concepcion, A. Corma, S. Iborra, M.J. Sabater, Chemicals from biomass: chemoselective reductive amination of ethyl levulinate with amines, ACS Catal. 5 (2015) 5812–5821.
[5] F. Robert, S. William, Z. Blossom, 1, 5-Dimethyl-2-Pyrrolidone, Org. Synth. 27 (1947) 28.
[6] W.C. Wilbur, L. Shilling, Making lactams by the vapor phase reductive amination of oxo carboxylic acid compounds, US Patent 3235562, 1966.
[7] A.S. Touchy, S.M.a.H. Siddiki, K. Kon, K. Shimizu, Heterogeneous Pt catalysts for reductive amination of levulinic acid to pyrrolidones, ACS Catal. 2 (2014) 3045–3050.
[8] Y. Wei, C. Wang, X. Jiang, D. Xue, J. Li, J. Xiao, Highly efficient transformation of levulinic acid into pyrrolidinones by iridium catalysed transfer hydrogenation, Chem. Commun. (2013) 5408–5410.
[9] Y. Wei, C. Wang, X. Jiang, D. Xue, Z.-T. Liu, J. Xiao, Catalyst-free transformation of levulinic acid into pyrrolidinones with formic acid, Green Chem. 16 (2014) 1093–1096.
[10] A. Ledoux, L. Sandjong Kuigwa, E. Framery, B. Andrioletti, A highly sustainable route to pyrrolidone derivatives −direct access to biosourced solvents, Green Chem. (2015).
[11] Y. Huang, J. Dai, X. Deng, Y. Qu, Q. Guo, Y. Fu, Ruthenium-catalyzed conversion of levulinic acid to pyrrolidines by reductive amination, ChemSusChem (2011) 1578–1581.
[12] Y. Ogiwara, T. Uchiyama, N. Sakai, Reductive Amination/Cyclization of keto acids using a hydrosilane for selective production of lactams versus cyclic amines by switching of the indium catalyst, Angew. Chem. Int. Ed. (2015) 1864–1867.
[13] C. Ortiz-Cervantes, M. Flores-Alamo, J.J. García, Synthesis of pyrrolidones and quinolines from the known biomass feedstock levulinic acid and amines, Tetrahedron Lett. 57 (2016) 766–771.
[14] J.J. Martínez, E. Nope, H. Rojas, M.H. Brijaldo, F. Passos, G. Romanelli, Reductive amination of furfural over me/SiO2-SO3H (Me: Pt Ir, Au) catalysts, J. Mol. Catal. A Chem. 392 (2014) 235–240.
[15] W. Yu, M. Liu, H. Liu, J. Zheng, Preparation of polymer-Stabilized noble metal colloids, J. Colloid Interface Sci. 210 (1999) 218–221.
[16] R. Lukeš, Z. Koblicová, K. Bláha, Über die reaktion der angelicalactone mit aminen, Collect. Czechoslov. Chem. Commun. 28 (1963) 2182–2198.
[17] M.J. Frisch, G.W. Trucks, H.B. Schlegel, G.E. Scuseria, G.A.J.R. Cheeseman, G. Scalmani, V. Barone, B. Mennucci, A.F. Petersson, H. Nakatsuji, M. Caricato, X. Li, H.P. Hratchian, M.E. Izmaylov, J. Bloino, G. Zheng, J.L. Sonnenberg, M. Hada, Y.H. K. Toyota, R. Fukuda, J. Hasegawa, M. Ishida, T. Nakajima, J.E.P.O. Kitao, H. Nakai, T. Vreven, J.A. Montgomery, V.N.F. Ogliaro, M. Bearpark, J.J. Heyd, E. Brothers, K.N. Kudin, A.R. Staroverov, R. Kobayashi, J. Normand, K. Raghavachari, J.M.M.J.C. Burant, S.S. Iyengar, J. Tomasi, M. Cossi, N. Rega, J.J.M. Klene, J.E. Knox, J.B. Cross, V. Bakken, C. Adamo, R.C.R. Gomperts, R.E. Stratmann, O. Yazyev, A.J. Austin, V.G.C. Pomelli, J.W. Ochterski, R.L. Martin, K. Morokuma, S.D. Zakrzewski, G.A. Voth, P. Salvador, J.J. Dannenberg, A.A.D. Daniels, Farkas, J.B. Foresman, J. V. Ortiz, J. Cioslowski, D.J. Fox, Gaussian Inc. Gaussian Inc. Wallingford CT, (2009).
[18] C. Steffen, K. Thomas, U. Huniar, A. Hellweg, O. Rubner, A. Schroer, TmoleX-a graphical user interface for TURBOMOLE, J. Comput. Chem. 31 (2010) 2967–2970.
[19] J. Tomasi, B. Mennucci, R. Cammi, Quantum mechanical continuum solvation models, Chem. Rev. 105 (2005) 2999–3093.
[20] W. Zhu, H. Yang, J. Chen, C. Chen, L. Guo, H. Gan, X. Zhao, Z. Hou, Efficient hydrogenolysis of cellulose into sorbitol catalyzed by a bifunctional catalyst, Green Chem. 16 (2014) 1534–1542.
[21] M.J. Sharif, P. Maity, S. Yamazoe, T. Tsukuda, Selective hydrogenation of nitroaromatics by colloidal iridium nanoparticles, Chem. Lett. 42 (2013) 1023.
[22] S.J. Morgan, R.H. Williams, J.M. Mooney, An XPS study of thin Pt and Ir silicide overlayer formation on Si(100)2X1 surfaces, Appl. Surf. Sci. 56–58 (56) (1992) 493—.
[23] A.K. Shukla, A.M. Kannan, M.S. Hegde, J. Gopalakrishnan, Effect of counter cations on electrocatalytic activity of oxide pyrochlores towards oxygen reduction/evolution in alkaline medium: an electrochemical and spectroscopic study, J. Power Sources 35 (1991) 163–173.
[24] P.P. Upare, J.-W. Yoon, M.Y. Kim, H.-Y. Kang, D.W. Hwang, Y.K. Hwang, H.H. Kung, J.-S. Chang, Chemical conversion of biomass-derived hexose sugars to levulinic acid over sulfonic acid-functionalized graphene oxide catalysts, Green Chem. 15 (2013) 2935.
[25] S. Hamoudi, S. Kaliaguine, Sulfonic acid-functionalized periodic mesoporous organosilicas, Stud. Surf. Sci. Catal. 146 (2002) 473–476.
[26] P.L. Anto, R.J. Anto, H.T. Varghese, C.Y. Panicker, D. Philip, a. G. Brolo, FT-IR, FT-Raman and SERS spectra of anilinium sulfate, J. Raman Spectrosc. 40 (2009) 1810–1815.
[27] R.G. Parr, R.G. Pearson, Absolute hardness: companion parameter to absolute electronegativity, J. Am. Chem. Soc. 105 (1983) 7512–7516.